Stem Cell Reports, Volume *7*

Supplemental Information

Distinctive Mesenchymal-Parenchymal Cell Pairings Govern B Cell Differentiation in the Bone Marrow

Vionnie W.C. Yu, Stefania Lymperi, Toshihiko Oki, Alexandra Jones, Peter Swiatek, Radovan Vasic, Francesca Ferraro, and David T. Scadden

Figure S1

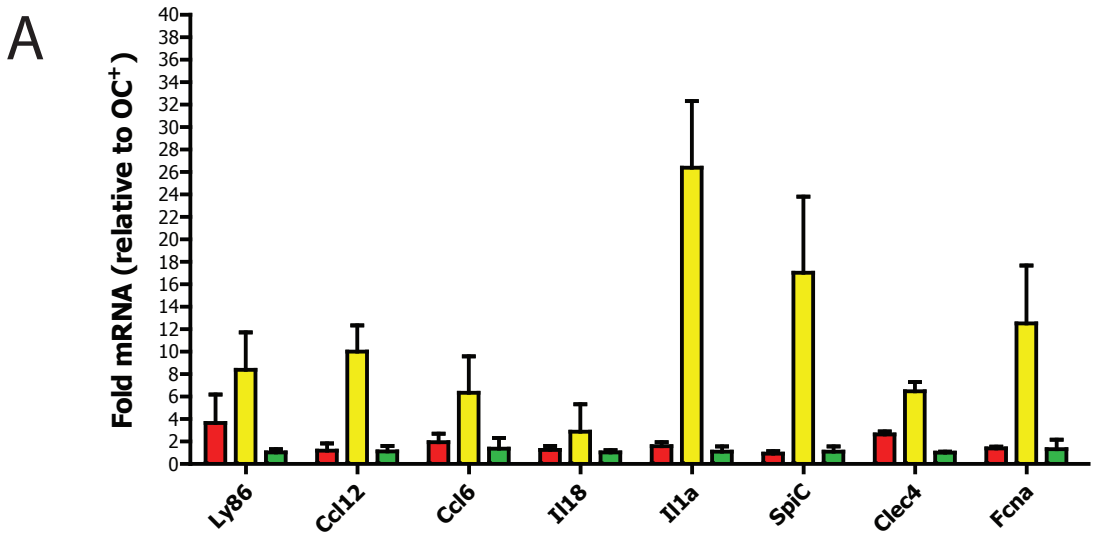
A
Fold mRNA (relative to OC+)
Ly86
Ccl12
Ccl6
Il18
Il1a
SpiC
Clec4
Fcna

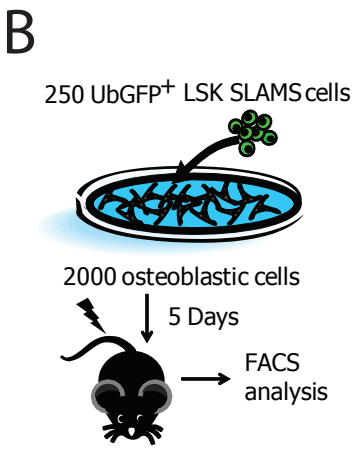
B
250 UbGFP+ LSK SLAMS cells
2000 osteoblastic cells
5 Days
FACS analysis

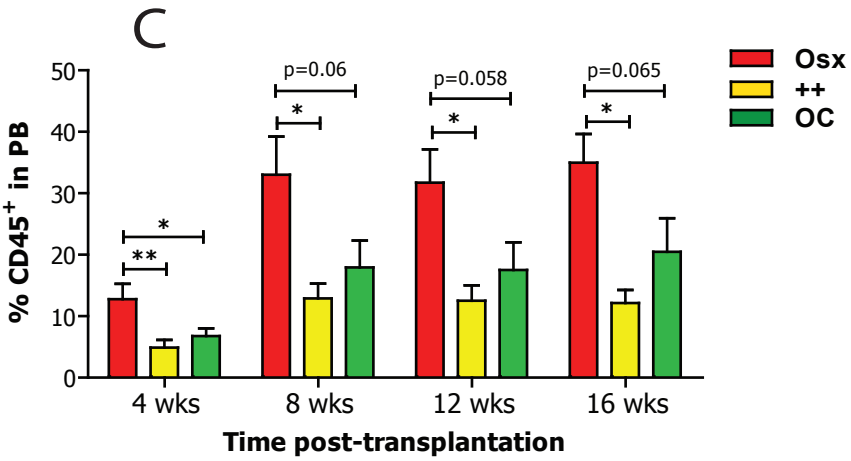
C
% CD45+ in PB
p=0.06
p=0.058
p=0.065
Osx
++
OC
4 wks
8 wks
12 wks
16 wks
Time post-transplantation

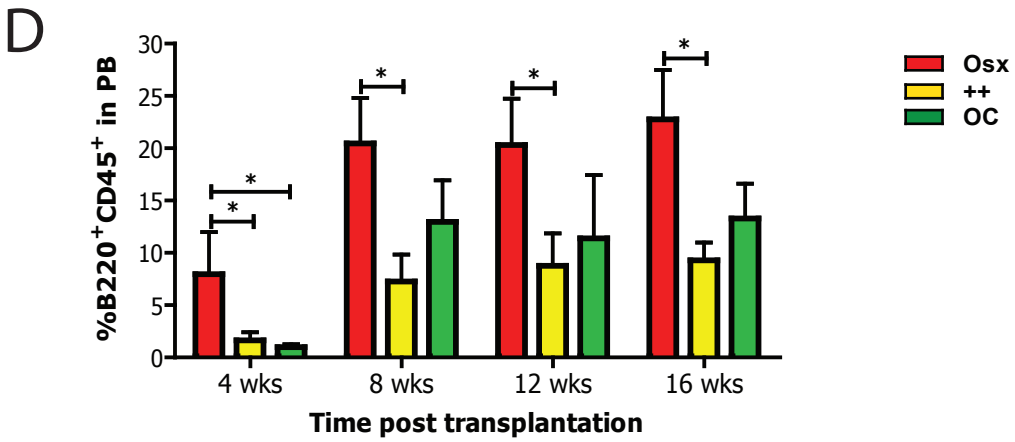
D
%B220+CD45+ in PB
Osx
++
OC
4 wks
8 wks
12 wks
16 wks
Time post transplantation

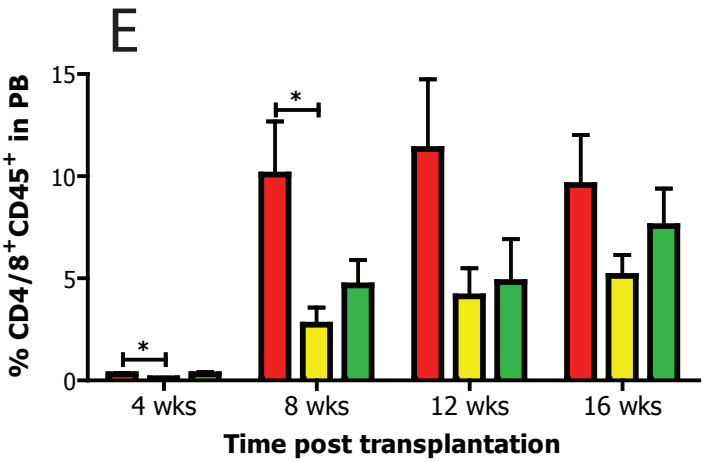
E
% CD4/8+CD45+ in PB
4 wks
8 wks
12 wks
16 wks
Time post transplantation

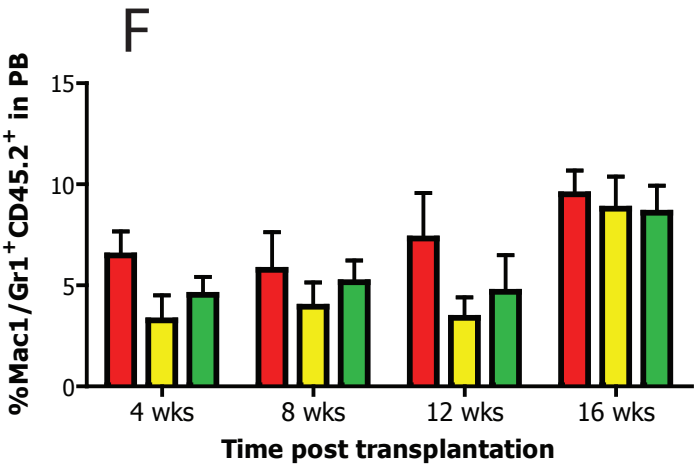
F
%Mac1/Gr1+CD45.2+ in PB
4 wks
8 wks
12 wks
16 wks
Time post transplantation

Figure S2

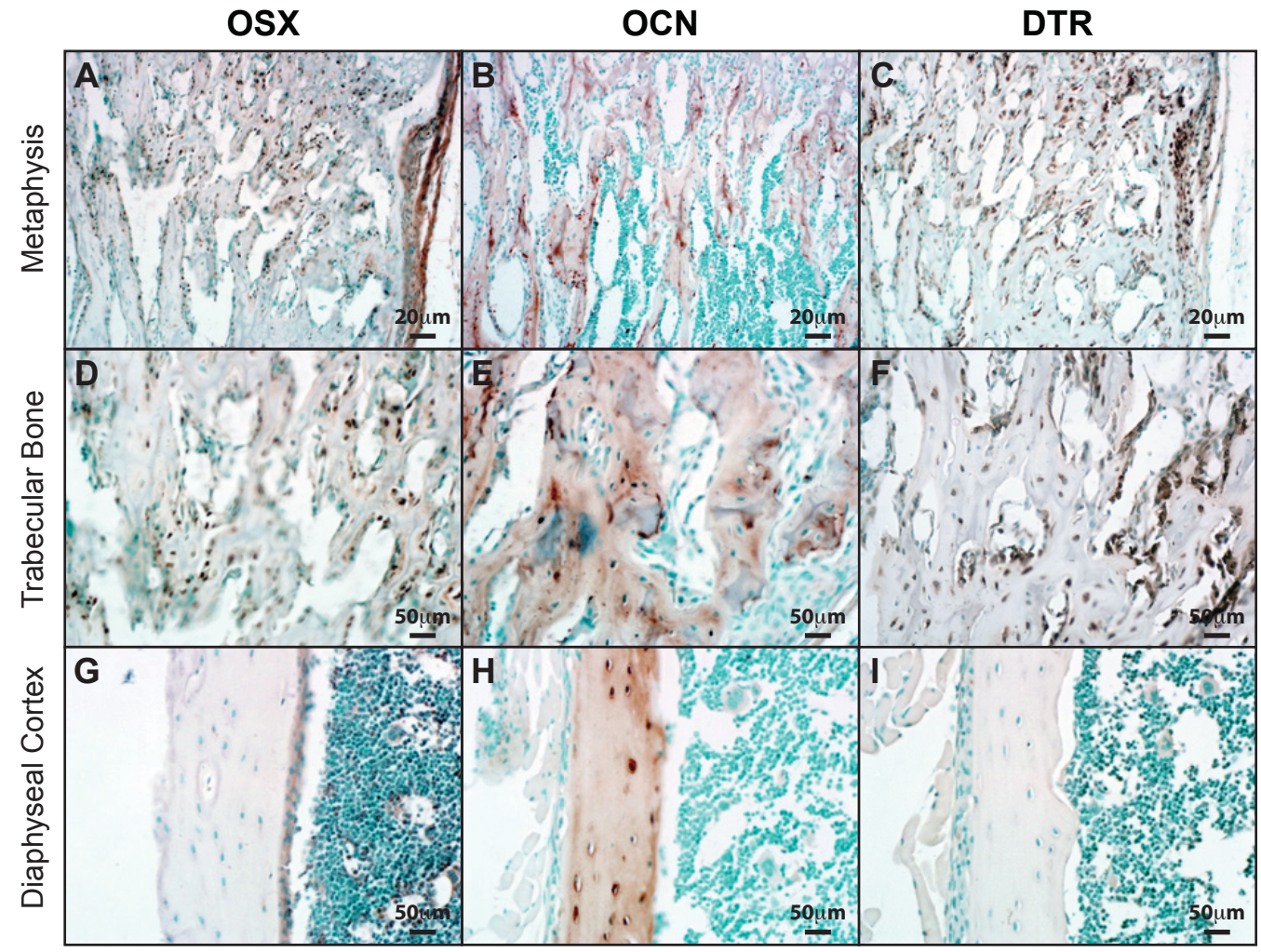
OSX
OCN
DTR
Metaphysis
Trabecular Bone
Diaphyseal Cortex
A
B
C
D
E
F
G
H
I
20μm
50μm

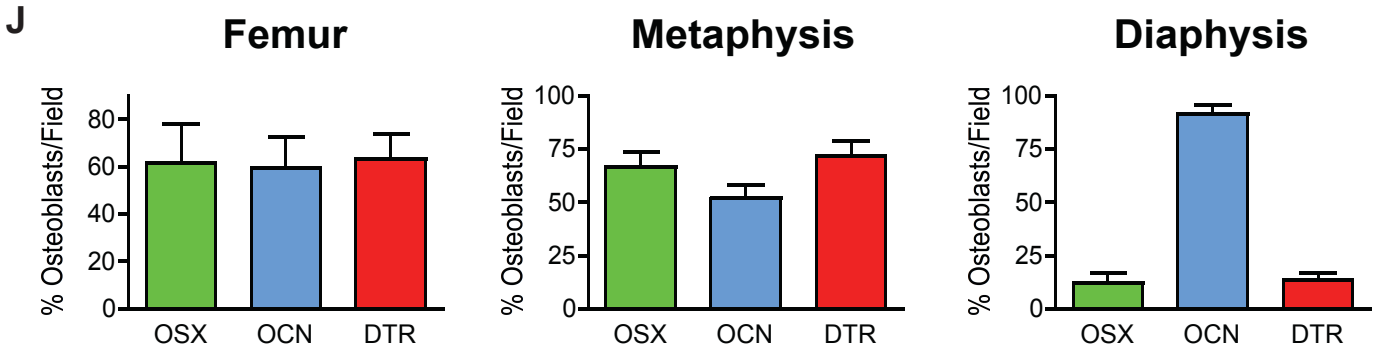
J
Femur
Metaphysis
Diaphysis
% Osteoblasts/Field
OSX
OCN
DTR

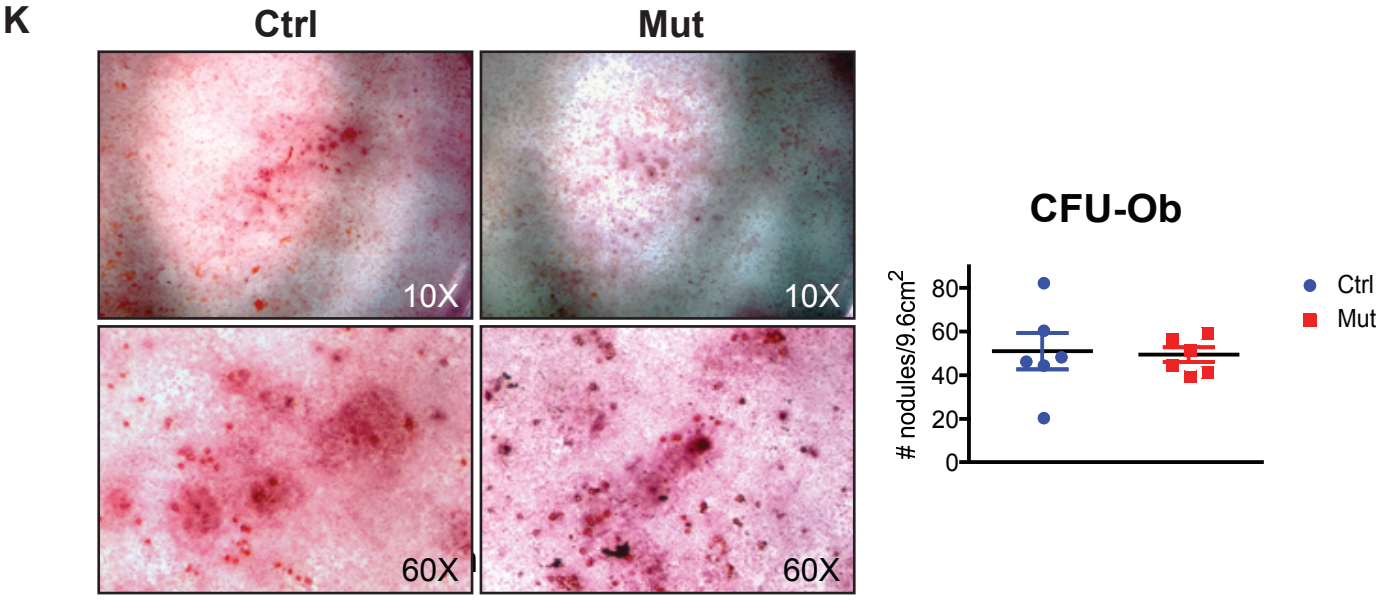
K
Ctrl
Mut
10X
60X
CFU-Ob
nodules/9.6cm2
Ctrl
Mut

Figure S3

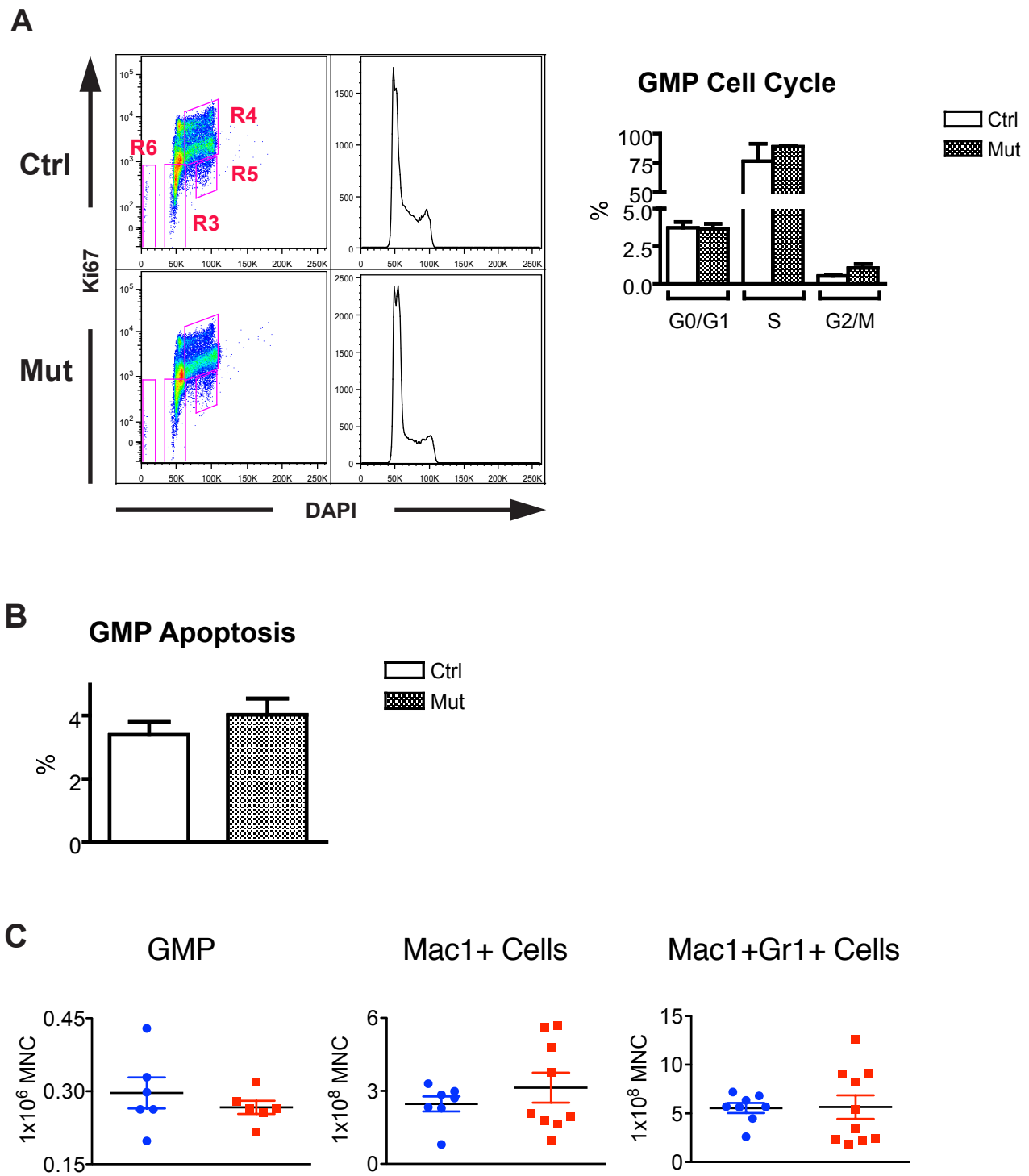
A
Ctrl
Mut
Ki67
DAPI
R3
R4
R5
R6
GMP Cell Cycle
Ctrl
Mut
%
G0/G1
S
G2/M
B
GMP Apoptosis
Ctrl
Mut
%
C
GMP
Mac1+ Cells
Mac1+Gr1+ Cells
1x10^6 MNC
1x10^8 MNC
1x10^8 MNC

Figure S4

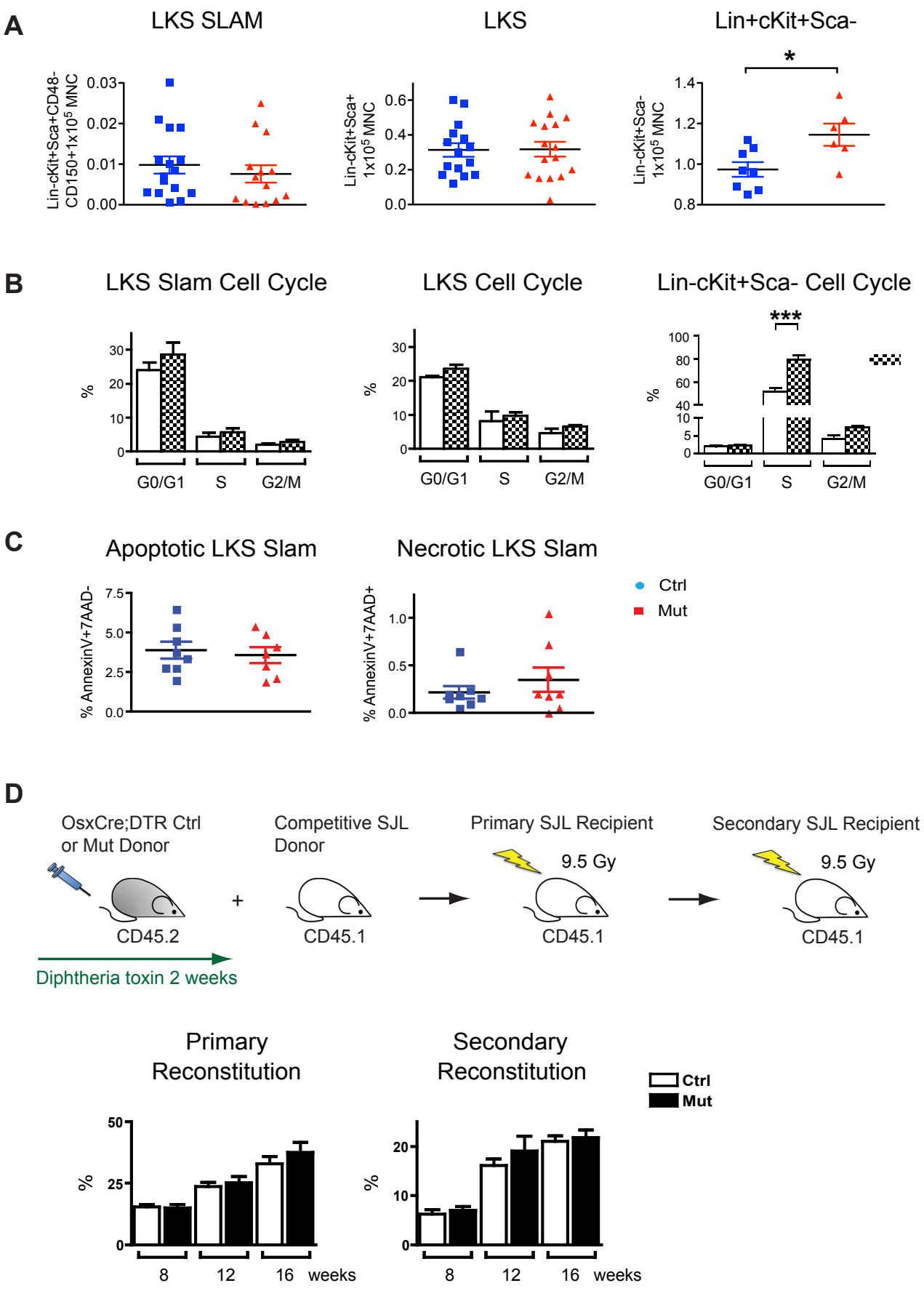
A
LKS SLAM
LKS
Lin+cKit+Sca-
Lin-cKit+Sca+CD48-CD150+1x10^5 MNC
Lin-cKit+Sca+ 1x10^5 MNC
Lin-cKit+Sca- 1x10^5 MNC
*
B
LKS Slam Cell Cycle
LKS Cell Cycle
Lin-cKit+Sca- Cell Cycle
***
%
G0/G1
S
G2/M
C
Apoptotic LKS Slam
Necrotic LKS Slam
% AnnexinV+7AAD-
% AnnexinV+7AAD+
Ctrl
Mut
D
OsxCre;DTR Ctrl or Mut Donor
Competitive SJL Donor
Primary SJL Recipient
Secondary SJL Recipient
9.5 Gy
CD45.2
CD45.1
Diphtheria toxin 2 weeks
Primary Reconstitution
Secondary Reconstitution
Ctrl
Mut
%
8
12
16
weeks

Figure S5

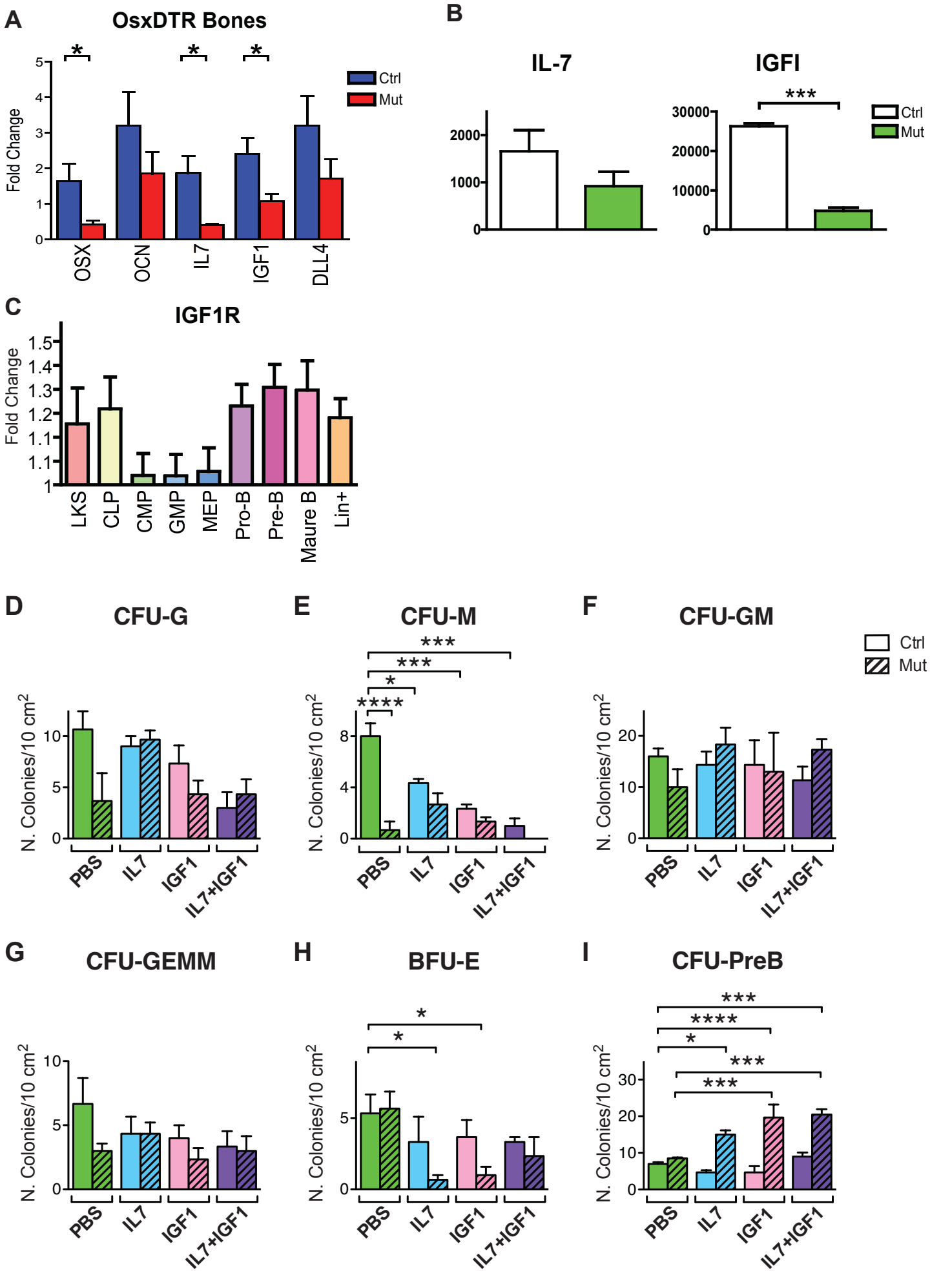
A
OsxDTR Bones
Fold Change
Ctrl
Mut
OSX
OCN
IL7
IGF1
DLL4
B
IL-7
IGFI
Ctrl
Mut
C
IGF1R
Fold Change
LKS
CLP
CMP
GMP
MEP
Pro-B
Pre-B
Maure B
Lin+
D
CFU-G
E
CFU-M
F
CFU-GM
Ctrl
Mut
N. Colonies/10 cm2
PBS
IL7
IGF1
IL7+IGF1
G
CFU-GEMM
H
BFU-E
I
CFU-PreB

Figure S6

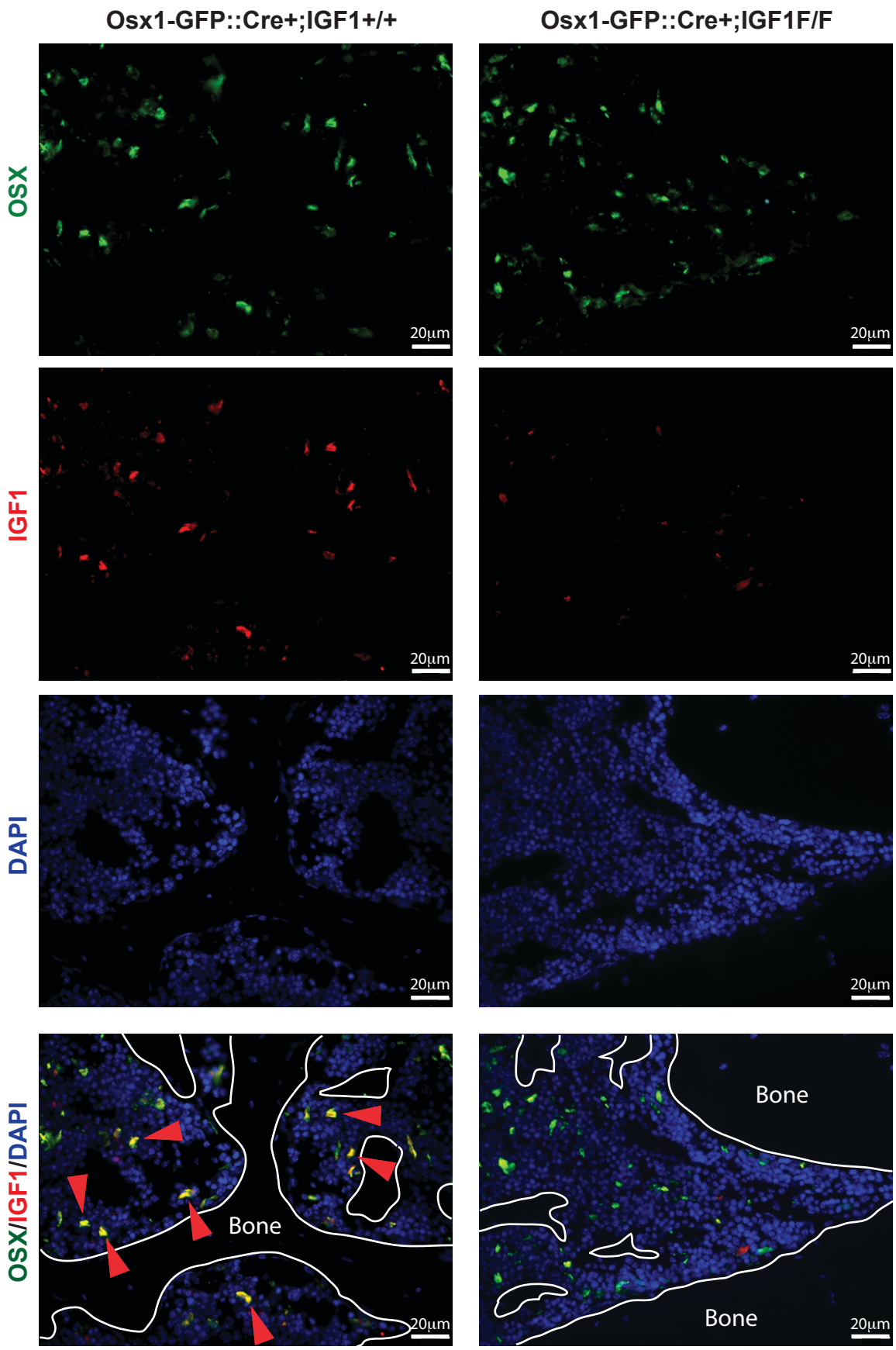
Osx1-GFP::Cre+;IGF1+/+
Osx1-GFP::Cre+;IGF1F/F
OSX
IGF1
DAPI
OSX/IGF1/DAPI
20μm
Bone
Bone
Bone

Figure S7

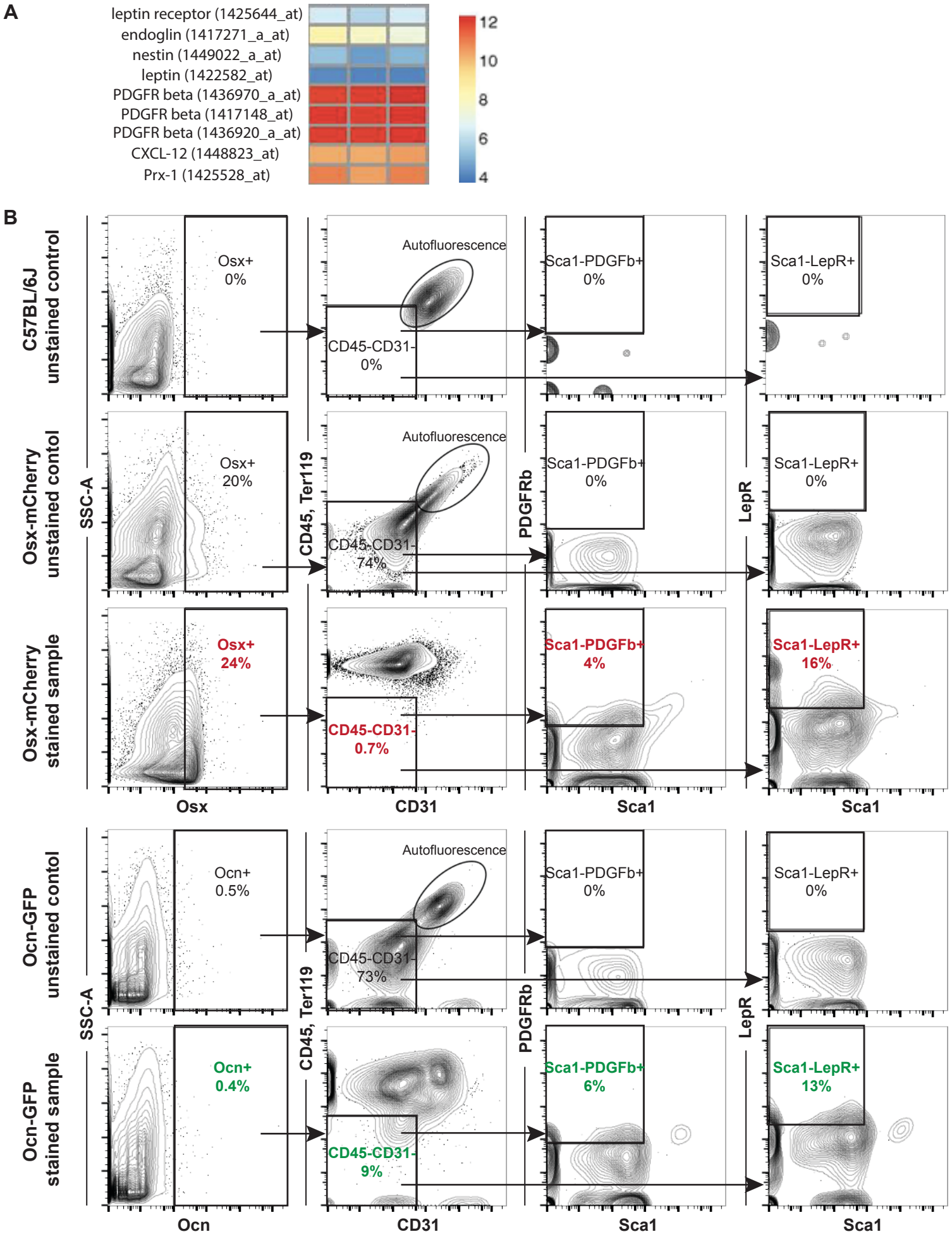
A
leptin receptor (1425644_at)
endoglin (1417271_a_at)
nestin (1449022_a_at)
leptin (1422582_at)
PDGFR beta (1436970_a_at)
PDGFR beta (1417148_at)
PDGFR beta (1436920_a_at)
CXCL-12 (1448823_at)
Prx-1 (1425528_at)
12
10
8
6
4
B
C57BL/6J unstained control
Osx-mCherry unstained contol
Osx-mCherry stained sample
Ocn-GFP unstained contol
Ocn-GFP stained sample
SSC-A
CD45, Ter119
PDGFRb
LepR
Osx+ 0%
Osx+ 20%
Osx+ 24%
Ocn+ 0.5%
Ocn+ 0.4%
Autofluorescence
CD45-CD31- 0%
CD45-CD31- 74%
CD45-CD31- 0.7%
CD45-CD31- 73%
CD45-CD31- 9%
Sca1-PDGFb+ 0%
Sca1-PDGFb+ 4%
Sca1-PDGFb+ 6%
Sca1-LepR+ 0%
Sca1-LepR+ 16%
Sca1-LepR+ 13%
Osx
Ocn
CD31
Sca1
Sca1

Table S1

Gene	OCN-1	OCN-2	OSX-1	OSX-2	fold change	difference of means	P value	OCN-1	OCN-2	"++_1"	"++_2"	fold change	difference of means
melanoma cell adhesion molecule	2614.03	2434.17	760.89	802.63	-3.2	-1726.14	0.045428	2614.03	2434.17	705.99	917.87	-3.09	-1697.76
potassium voltage-gated channel, Isk-related subfamily, gene 3	584.83	530.25	28.96	84.44	-9.9	-501.45	0.007775	584.83	530.25	15.59	64.84	-14.17	-518.46
quinolinate phosphoribosyltransferase	862.77	1082.29	179.06	393.06	-3.41	-687.32	0.047214	862.77	1082.29	225.45	163.24	-4.96	-776.68
cadherin EGF LAG seven-pass G-type receptor 1	131.53	121.09	32.03	17.72	-4.7	-99.22	0.025416	131.53	121.09	50.81	27.19	-3.2	-86.73
C-type lectin domain family 4, member n	164.31	465.13	1244.34	1489.72	4.35	1053.4	0.035361	164.31	465.13	2676.55	2894.1	8.9	2481.26
CD4 antigen	26.18	79.22	258.76	311.45	5.4	233.65	0.030946	26.18	79.22	962.87	637.58	15.03	745.23
vanin 3	9.55	3.7	60.45	55.29	9.79	52.56	0.045097	9.55	3.7	121.16	62.92	15.35	85.76
protein kinase inhibitor beta, cAMP dependent, testis specific	16.71	11.99	54.3	63.92	4.18	44.02	0.048028	16.71	11.99	87.28	84.6	6.23	72.39
platelet/endothelial cell adhesion molecule 1	688.1	585.33	50.45	183.64	-5.44	-517.86	0.030341	688.1	585.33	37.18	137.18	-7.29	-547.48
macrophage scavenger receptor 1	51.6	84.49	416.62	409.67	6.1	345.54	0.00554	51.6	84.49	550.15	379.61	6.86	396.93
interleukin 1 receptor antagonist	24.38	73.75	257.25	298.67	5.69	229.89	0.023307	24.38	73.75	352.77	625.09	9.98	440.26
GTPase, IMAP family member 4	273.36	237.74	16.79	80.8	-5.24	-205.02	0.042566	273.36	237.74	23.77	73.91	-5.22	-204.84
similar to Tetraspanin-15 (Tspan-15)	398.38	362.18	107.77	33.16	-5.46	-312.96	0.030316	398.38	362.18	95.33	87.05	-4.27	-293.35
membrane-spanning 4-domains, subfamily A, member 7	637.91	1286.01	4742.51	3904.73	4.51	3367.72	0.030333	637.91	1286.01	6369.65	5455.16	6.16	4949.11
macrophage scavenger receptor 1	42.14	75.23	263.2	283.38	4.59	213.05	0.01288	42.14	75.23	268.2	377.09	5.47	265.13
osteoclast associated receptor	1313.99	1109.17	74.7	14.4	-27.08	-1166.58	0.039424	1313.99	1109.17	56.21	4.65	-41.37	-1182.03
C-type lectin domain family 4, member n	183.82	535.22	1308.63	1569.1	4.01	1081.82	0.045017	183.82	535.22	2907.4	3021.55	8.29	2622.11
GTPase, IMAP family member 6	1301.48	1208.93	212.61	473.67	-3.7	-920.34	0.04125	1301.48	1208.93	393.53	465.61	-2.93	-830.86
Ras interacting protein 1	460.94	564.74	38.16	123.61	-6.37	-430.88	0.028213	460.94	564.74	43.97	160.51	-5.01	-409.06
GATA binding protein 2	563.37	503.42	198.21	80.36	-3.81	-390.66	0.043908	563.37	503.42	129.35	99.25	-4.66	-416.01
ATP-binding cassette, sub-family C (CFTR/MRP), member 3	589.53	562.34	2201.91	2167.21	3.79	1612.97	0.014755	589.53	562.34	4228.47	2577.05	5.89	2823.78
epoxide hydrolase 2, cytoplasmic	509.1	614.63	165.99	120.24	-3.93	-417.83	0.04546	509.1	614.63	151.82	156.08	-3.66	-407.13
toll-like receptor 1	18.25	44.68	227.1	203.06	6.99	184	0.019714	18.25	44.68	614.24	348.54	15.7	451.52
CD86 antigen	32.2	99.92	483.51	450.26	7.19	404.45	0.01511	32.2	99.92	1348.84	1206.46	19.58	1213.37
interleukin 1 receptor antagonist	364.91	901.89	3243.86	3195.64	5.08	2582.6	0.03401	364.91	901.89	3913.95	4386.25	6.61	3550.99
endothelial cell-specific adhesion molecule	1082.55	1212.24	61.34	250.81	-7.43	-994.47	0.01704	1082.55	1212.24	92.7	332.37	-5.44	-937.84

Table S2

Up in Osx

Name	pValue
Cell adhesion_Cell-matrix glycoconjugates	0.001674326
Cholesterol Biosynthesis	0.002165012
Neurophysiological process_Receptor-mediated axon growth repulsion	0.002730821
Cell cycle_Nucleocytoplasmic transport of CDK/Cyclins	0.003334932
Transport_RAN regulation pathway	0.005518031
Cell cycle_ESR1 regulation of G1/S transition	0.017937452
G-protein signaling_RhoA regulation pathway	0.018982992
G-protein signaling_Regulation of p38 and JNK signaling mediated by G-proteins	0.024581384
Development_Hedgehog signaling	0.033396544
Mechanisms of CFTR activation by S-nitrosoglutathione (normal and CF)	0.033396544

Up in ++

Name	pValue
Immune response_Alternative complement pathway	1.06177E-16
Immune response_Lectin induced complement pathway	1.12451E-13
Immune response_Classical complement pathway	2.44826E-13
Immune response_Histamine signaling in dendritic cells	1.12387E-06
Atherosclerosis_Role of ZNF202 in regulation of expression of genes involved in Atherosclerosis	2.68065E-06
Bacterial infections in CF airways	3.14756E-06
Niacin-HDL metabolism	1.18712E-05
Apoptosis and survival_TNFR1 signaling pathway	0.000104563
Immune response_Fc gamma R-mediated phagocytosis in macrophages	0.000130412
Immune response_Antigen presentation by MHC class II	0.000271238

Up in Ocn

Name	pValue
Development_Transcription regulation of granulocyte development	6.36773E-05
Cell adhesion_Plasmin signaling	0.001222437
Cell adhesion_Cell-matrix glycoconjugates	0.001670272
Signal transduction_cAMP signaling	0.001670272
Development_Regulation of epithelial-to-mesenchymal transition (EMT)	0.001707236
Transport_ACM3 in salivary glands	0.002221033
Immune response_PGE2 in immune and neuroendocrine system interactions	0.002650867
Regulation of lipid metabolism_Regulation of lipid metabolism by niacin and isoprenaline	0.003134584
Cell adhesion_Endothelial cell contacts by non-junctional mechanisms	0.00401394
Cell adhesion_Endothelial cell contacts by junctional mechanisms	0.005055688

Supplemental Figure Legends

Figure S1: Osteolineage subpopulations differ in their capacity to support hematopoietic lineage-specific reconstitution, Related to Figure 1. (**A**) RT-PCR validation of candidate genes selected from the microarray comparison of *Ocn*$^+$, ++ and *Osx*$^+$ cells. Columns are mean ± s.e.m. Fold changes are relative to GAPDH (ΔΔCT method). (**B**) Two hundred and fifty flow sorted HSPCs were co-cultured with 2000 Ocn$^+$, ++, or Osx$^+$ cells flow sorted from the OsxCre$^+$;Rosa-mCh$^+$;Ocn:Topaz triple transgenic mice. UbGFP$^+$=ubiquitin GFP positive cell. (**C**) After 5 days of co-culture with Ocn$^+$, ++ or Osx$^+$ cells, CD45.2 HSPCs were injected into lethally irradiated CD45.1 recipients. At 4, 8, 12, and 16 weeks post-transplantation, percentage of reconstituted CD45.2 donor cells was determined by FACS analysis. Column represents mean±s.e.m., n=8, *p<0.05, **p<0.01. (**D**) Percentages of donor-derived B cells (B220$^+$), (**E**) T cells (CD4/8$^+$) and (**F**) macrophages/monocytes (Mac1/Gr1$^+$) in the peripheral blood of CD45.1 recipients injected with CD45.2 HSPCs. (**A-F**) Experiment repeated once. Columns represent mean±s.e.m., n=8/group, *p<0.05. Error bars represent ±s.e.m.

Figure S2: Targeted ablation of Osx$^+$ cells did not affect mesenchymal progenitor cells, Related to Figure 2. (**A-I**) To assess whether the correct osteolineage cell population was targeted for cell death, immunohistochemistry was performed on mutant OsxCre;iDTR bones without toxin treatment using anti-Osx, anti-Ocn, and anti-hbEGF antibody, which recognizes the diphtheria toxin receptor (DTR).Expression of the DTR highly correlated with the expression of Osx but not Ocn. (**J**) Histomorphometric quantification of the number of osteoblasts expressing Osx, Ocn, and DTR in femurs. The number of osteolineage cells expressing Osx, Ocn, and DTR were similar in the overall femur and in the metaphysis, however, the expression pattern changed dramatically in the diaphysis of the long bone, with Osx and DTR expressions correlated with each other in the OsxCre;iDTR model. (**K**) Colony forming assay-osteoblast (CFU-Ob) did not show any changes in the number of mesenchymal progenitors in the bone

marrow of OsxCre;iDTR mutants compared to controls. (**A-K**) Two independent experiments, n=6-10/group. Error bars represent ±s.e.m.

Figure S3: Cell cycle and apoptotic analysis of OsxCre;iDTR GMPs, Related to Figure 3. **(A)** GMPs harvested form OsxCre;iDTR control and mutant femurs were stained with intracellular Ki67 and DAPI stains to reveal cell cycle status and apoptotic cells. R3 = G0/G1, R4 = S, and R5 = G2/M phase of cell cycle. R6 = apoptotic cells at G0/G1 phase. (**B**) GMP apoptosis was also assessed by annexinV and 7AAD staining. (**C**) Upon i.p. injection of indomethacin, the number of GMPs, $Mac1^+$, and $Mac1^+Gr1^+$ cells in the OsxCre;iDTR mutant mice were comparable to controls. (**A-C**) Two independent experiments, n=6-9/group. Error bars represent ±s.e.m.

Figure S4: Short-term deletion of Osx^+ cells did not affect HSC reconstitution, Related to Figure 3. (**A-C**) No change in LKS SLAM and LKS cell number, proliferation, and apoptosis was observed in the OsxCre;iDTR mutant animals, but an increase in the number of $Lin^{lo}cKit^+Sca^-$ progenitor cells was detected (**A**), likely due to more cells at the S phase of the cell cycle (**B**). Three independent experiments, n=6-15/group. (**D**) Competitive primary and secondary transplantations did not reveal any reconstitutional defect of HSCs derived from OsxCre;iDTR mutants. Two independent experiments, n=20/group. Error bars represent ±s.e.m.

Figure S5: Osx^+ cells produce IL7 and IGF1 to regulate B cell differentiation and rescue the *in vitro* OsxCre;iDTR mutant phenotype, Related to Figures 4, 6 and 7. (A) Transcript expression of IL7 and IGF1 were significantly reduced in OsxCre;iDTR mutant bones. (**B**) Bone marrow sera from OsxCre;iDTR mutant and control mice were subjected to a cytokine array to measure factors released by Osx^+ cells into the bone marrow microenvironment. While IL7 protein level was partially but non-significantly affected, IGF1 was remarkably lower in the

OsxCre;iDTR mutant sera compared to control littermates. (**C**) Quantitative PCR showed that expression of the IGF1 receptor was high in flow sorted LKS, CLP, pro-B, pre-B, mature B, and lineage$^+$ cells but low in CMP, GMP, and MEP cells. Note that data are not statistically significant. (**A-C**) Two independent experiments, n=6-8/group. Error bars represent ±s.e.m. (**D-I**) Hematopoietic stem and progenitor cells were harvested from OsxCre;iDTR control and mutant mice and plated in methycellulose-containing media for CFU assays. Cells were grown with (1) no supplement, (2) IL7, (3) IGF1, or (4) IL7+IGF1 for 14 days and enumerated for CFU-G (**D**), CFU-M (**E**), CFU-GM (**F**), CFU-GEMM (**G**), BFU-E (**H**), and CFU-PreB (**I**). Both IL7 and IGF1 promoted pre-B colony formation and the effect was additive (**I**). No positive regulation on the differentiation of hematopoietic progenitors of other lineages was found (**D-H**). Cells were plated in triplicates and the experiment was repeated twice. Error bars represent ±s.e.m.

Figure S6: Specific deletion of IGF1R in Osx$^+$ cells in Osx1-GFP::Cre$^+$;IGF1$^{F/F}$ mouse model, Related to Figure 6. Immunohistochemistry was performed on Osx1-GFP::Cre$^+$;IGF1$^{F/F}$ and Osx1-GFP::Cre$^+$;IGF1$^{+/+}$ bone sections using antibodies targeting Osx (green), IGF1 (red), and counterstained with DAPI nucleus stain (blue). Red arrowheads point to cells that co-expressed Osx and IGF1 in wild type animals. Representative images were shown. Two independent experiments, n=5/group.

Figure S7: Expression of stromal cell markers on Osx$^+$ and Ocn$^+$ populations, Related to Figure 1. (**A**) Gene expression levels of various stromal cell markers on Osx$^+$ cells as measured by microarray. Data represent triplicates. (**B**) Characterization of CD45$^-$CD31$^-$Sca1$^-$PDGF$^+$ and CD45$^-$CD31$^-$Sca1$^-$LepR$^+$ expression on Osx$^+$ cells and Ocn$^+$ cells by flow cytometry, using Osx-mCherry and Ocn-GFP transgenic models, respectively. Representative flow plots are illustrated. Data represent averaged percentages, n=4/group.

Supplemental Table Legends

Table S1: Table showing the list of top 25 differentially expressed genes between Osx^{+}, ++, and Ocn^{+} cells using dChip gene analysis, Related to Figure 1.

Table S2: GeneGo Pathway Maps show genes upregulated in Osx^{+}, ++, and Ocn^{+} cells, Related to Figure 1. "Statistically significant maps" were sorted after enrichment analysis. Analysis includes matching gene IDs of possible targets for the "common", "similar" and "unique" sets with gene IDs in functional ontologies in MetaCore. The probability of a random intersection between a set of IDs given the size of the target list with ontology entities is estimated in p−value of hyper geometric intersection. The lower p−value means higher relevance of the entity to the dataset, which shows in higher rating for the entity.